

# A log-quadratic relation for predicting supermassive black hole masses from the host bulge Sérsic index

Alister W. Graham<sup>1</sup>

*Mount Stromlo and Siding Spring Observatories, Australian National University, Private Bag, Weston Creek PO, ACT 2611, Australia.*

Simon P. Driver<sup>2</sup>

*School of Physics & Astronomy, University of St Andrews, North Haugh, St Andrews, Fife, KY16 9SS, UK*

## ABSTRACT

We reinvestigate the correlation between black hole mass and bulge concentration. With an increased galaxy sample (totalling 27), updated estimates of galaxy distances, black hole masses, and Sérsic indices  $n$  — a measure of concentration — we perform a least-squares regression analysis to obtain a relation suitable for the purpose of predicting black hole masses in other galaxies. In addition to the linear relation,  $\log(M_{\text{bh}}) = 7.81(\pm 0.08) + 2.69(\pm 0.28) \log(n/3)$  with  $\epsilon_{\text{intrinsic}} = 0.31_{-0.07}^{+0.09}$  dex, we investigated the possibility of a higher order  $M_{\text{bh}}-n$  relation, finding the second order term in the best-fitting quadratic relation to be inconsistent with a value of zero at greater than the 99.99% confidence level. The optimal relation is given by  $\log(M_{\text{bh}}) = 7.98(\pm 0.09) + 3.70(\pm 0.46) [\log(n/3)] - 3.10(\pm 0.84) [\log(n/3)]^2$ , with  $\epsilon_{\text{intrinsic}} = 0.18_{-0.06}^{+0.07}$  dex and a total absolute scatter of 0.31 dex. Extrapolating the quadratic relation, it predicts black holes with masses of  $\sim 10^3 M_{\odot}$  in  $n = 0.5$  dwarf elliptical galaxies, compared to  $\sim 10^5 M_{\odot}$  from the linear relation, and an upper bound on the largest black hole masses in the local universe, equal to  $1.2_{-0.4}^{+2.6} \times 10^9 M_{\odot}$ .

In addition, we show that the nuclear star clusters at the centers of low-luminosity elliptical galaxies follow an extrapolation of the same quadratic relation — strengthening suggestions for a possible evolutionary link between supermassive black holes and nuclear star clusters. Moreover, we speculate that the merger of two such nucleated galaxies, accompanied by the merger and runaway collision of their central star clusters, may result in the late-time formation of some supermassive black holes.

Finally, we predict the existence of, and provide equations for, an  $M_{\text{bh}}-\mu_0$  relation, in which  $\mu_0$  is the (extrapolated) central surface brightness of a bulge.

*Subject headings:* black hole physics — galaxies: bulges — galaxies: fundamental parameters — galaxies: structure

## 1. Introduction

While perhaps not surprising to AGN-astronomers, over the past five to ten years, the notion that a supermassive black hole (SMBH;  $M_{\text{bh}} \geq 10^6 M_{\odot}$ ) resides at the heart of every significantly large

( $M_{\text{bulge}} \geq 10^9 M_{\odot}$ ) galaxy bulge, even inactive bulges, has changed from a dubious idea to a mainstream belief. Support for the tide-of-opinion change has, in part, arisen from studies of our own galaxy. Schödel (2003) and Ghez et al. (2005, and references therein, see also Broderick & Narayan 2006) have shown that the mass required inside of the innermost resolved volume of the Milky Way is sufficiently large that it rules out alternatives to

<sup>1</sup>Corresponding Author: Graham@mso.anu.edu.au

<sup>2</sup>Scottish Universities Physics Alliance (SUPA).

a SMBH, such as a cluster of dead stars or stellar mass black holes which, if they did once exist, have surely now merged to form a single, massive object (e.g., Miller 2006). Although there is only one other sufficiently well resolved galaxy where such a conclusion can be drawn, NGC 4258 (Miyoshi et al. 1995), it seems reasonable to accept that the dark concentrations of mass at the centers of other galaxies are also SMBHs, and we adopt this convention, or at least terminology, here.

Roughly some three dozen galaxies are close enough that their central, SMBH mass has been measured directly through its influence on the motion of the surrounding gas and stars (Kormendy & Gebhardt 2001; Merritt & Ferrarese 2001a; Ferrarese & Ford 2005, their Table II)<sup>1</sup>. To acquire the mass of the central dark object in other (inactive) galaxies requires an alternative approach, and a number of indirect means to do so have been proposed (e.g., Ferrarese & Merritt 2000; Gebhardt et al. 2000; Marconi & Hunt 2003; Novak, Faber & Dekel 2006).

Perhaps the most often used relation — due to the small level of scatter ( $\sim 0.3$  dex) — is the  $M_{\text{bh}}-\sigma$  relation (Ferrarese & Merritt 2000; Gebhardt et al. 2000). With an equivalent level of scatter, and the advantage of requiring only galaxy images rather than spectra, is the  $M_{\text{bh}}-n$  relation (Graham et al. 2001, 2003a), where  $n$  is a measure of the concentration of the stars within the bulge. More precisely,  $n$  is the inverse exponent from the best-fitting Sérsic (1963)  $R^{1/n}$  light-profile (see Graham & Driver 2005 for a review of this model). Other relations, often reported to have more scatter than the above two relations, are the  $M_{\text{bh}}-L$  and the  $M_{\text{bh}}-M_{\text{bulge}}$  relations (Kormendy 1993; Magorrian et al. 1998). Although, recent studies which have excluded the disk-dominated spiral galaxies (e.g., McLure & Dunlop 2002), or used only the bulge luminosity from the disk galaxies after performing an accurate bulge/disk decomposition (e.g., Erwin et al. 2002; Marconi & Hunt 2003) have obtained a relationship with a similarly low level of scatter (see also Häring & Rix 2004). All of these empirical relations can be, and indeed must be, used to constrain any *complete* theory

<sup>1</sup>We do not use the eight galaxies listed in part two of Table II from Ferrarese & Ford 2005 for which the SMBH masses might be in error.

or model of galaxy/SMBH co-evolution. Furthermore, all of these relations can be used to gauge the mass of SMBHs in other galaxies.

In this paper we use the Sérsic index  $n$ , together with updated SMBH masses (Section 2), to derive the first  $M_{\text{bh}}-n$  relation constructed for the purpose of predicting  $M_{\text{bh}}$  in other galaxies (Section 3). This relation may differ from the intrinsic, astrophysical relation presented in Graham et al. (2003a) due to the different method of regression that is required. Armed with such a relation, one requires only images — which need not even be photometrically calibrated — to predict accurate SMBHs in other galaxies. Additional advantages with the use of a global measure such as  $n$ , are that it is not heavily affected by possible kinematical sub-structure at the center of a bulge, nor by rotational velocity or vertical dispersion of an underlying disk, nor aperture corrections. Furthermore, the quantity  $n$  is cheap to acquire in terms of telescope time and unlike absolute magnitudes and masses, it does not depend on galaxy distance nor an uncertain mass-to-light ratio.

As noted in Graham et al. (2001), there is no *a priori* reason to presume that the relation between  $\log M_{\text{bh}}$  and  $\log n$  is linear, and we therefore explore the suitability of a quadratic equation. In so doing, we find the second order term is inconsistent with a value of zero at the 99.99% confidence level (Section 3.2). Implications at the low- and high- $n$  end of the relation are discussed, relative to the optimal linear fit.

In a forthcoming paper we will apply this quadratic relation to the Millennium Galaxy Catalog (Liske et al. 2003; Cross et al. 2004; Driver et al. 2006) containing 10 095 galaxies — which have been modeled with a Sérsic-bulge plus exponential-disk (Allen et al. 2006) — to determine the local supermassive black hole mass function (e.g., Salucci et al. 1999; Yu & Tremaine 2002; Granato et al. 2004; Shankar et al. 2004) and space density in both early- and late-type galaxies.

In Section 4 we expand the  $M_{\text{bh}}-n$  diagram into an  $M_{\text{mco}}-n$  diagram, where  $M_{\text{mco}}$  is the mass of the central compact object, which may be a SMBH or a nuclear star cluster. We show that the nuclear star clusters in early-type galaxies appear to follow the curved  $M_{\text{bh}}-n$  relation defined by galaxies with SMBHs, and we discuss some of the implica-

tions this may entail. In Section 5 we show that our  $M_{\text{bh}}-n$  relation is independent of the Hubble constant.

Given there are now several relations between SMBH mass and the properties the host bulge, in Section 6 we briefly present some musings as to what may be the fundamental primary relation. In this section we derive a new set of equations relating the SMBH mass to the (extrapolated) central surface density of the host bulge. Finally, in Section 7 we provide a brief summary of the paper.

## 2. Data for the $M_{\text{bh}}-n$ relation

Our sample is comprised of the 21 galaxies used in Graham et al. (2001) plus an additional six new galaxies.

A discussion of the original galaxy light-profiles can be found in Erwin et al. (2002), see also Trujillo et al. (2004). Due to updated galaxy distances and SMBH mass measurements, and a refined analysis of the major-axis light-profiles, some of the 27 data points (14 E and 13 S0/Sp) given in Table 1 are slightly different to those published in Graham et al. (2001, their table 1) and shown in Graham et al. (2003a, their figure 1). However, only for two galaxies has the Sérsic index changed by more than 20% — the typical uncertainty on this index (e.g., Caon, Capaccioli, & D’Onofrio 1993). We briefly comment on these two galaxies here and present their new Sérsic fits in Appendix A.

Although the bulge of the Milky Way is nowadays recognised as having an exponential ( $n = 1$ ) light-profile, we have fitted the near-infrared data from Kent, Dame, & Fazio (1991) and report an index of  $n = 1.32$  rather than exactly 1. The second galaxy in question is NGC 4564. Subsequent to the analysis in Trujillo et al. (2004), NGC 4564 is now recognized as an S0 galaxy that was mis-classified as an E galaxy. An  $R^{1/n}$ -bulge plus exponential-disk decomposition has therefore been performed. This resulted in its bulge Sérsic index  $n$  increasing from 2.1 to 3.2.

Four of the six new galaxies are listed in Ferrarese & Ford (2005) (NGC 3115, 4486, 4649, 4697) and our Sérsic fits to their light-profiles are also presented in Appendix A. In addition, we have used the bulge/disk decomposition shown in Graham (2002) for the supposedly “compact Ellipti-

cal” galaxy NGC 221 (M32), which was not included in our original paper. We have also been able to include NGC 1399 (Houghton et al. 2006), which previously had no direct SMBH mass estimate. This galaxy’s light-profile has been modeled in D’Onofrio, Capaccioli, & Caon (1994) and we adopt their Sérsic index having obtained the same value from our own fitting of their data.

Despite our attempt to include all of the lowest and highest mass SMBHs, as these data points can have substantial weight on any fitted relation, we have not included the peculiar elliptical galaxy IC 1459 due to uncertainty on both its SMBH mass and its Sérsic index  $n$ . This galaxy displays clear signs of past interaction, evidenced by stellar tidal tails (Malin 1985) and stellar shells and ripples at large radii (Forbes & Reitzel 1995). Due to its unrelaxed, disturbed morphology, its light-profile is not well fitted with an  $R^{1/n}$  model. It also possesses a fast counter-rotating stellar core. While the stellar dynamics of the core suggest a SMBH mass of  $2.6 \times 10^9 M_{\odot}$ , the gas dynamics reveal the mass could be as low as  $3.5 \times 10^8 M_{\odot}$  (Cappellari et al. 2002).

The upper section of Table II in Ferrarese & Ford (2005) lists 25 galaxies with SMBH masses derived from resolved dynamical studies. A further five galaxies in this list have marginally resolved mass estimates, with  $0.39 < r_{\text{sphere of influence}}/r_{\text{resolved}} < 0.92$ . Aside from IC 1459, we are only missing quality  $R$ -band images for three of these 30 galaxies: NGC 3608, NGC 5128 (Centaurus A) and the relatively distant ( $z = 0.056$ ) galaxy Cygnus A.

Most of our 27 galaxies have distances from Tonry et al. (2001), and updated SMBH mass estimates have come from Tremaine et al. (2002), with exceptions noted in Table 1. Three galaxies in our sample do not have ‘Surface Brightness Fluctuation’ distance measurements in Tonry et al. (2001). For the relatively distant galaxies NGC 6251 and NGC 7052, we used their heliocentric velocities (Wegner et al. 2003) and a Hubble constant  $H_0 = 73 \text{ km s}^{-1} \text{ Mpc}^{-1}$  (Blakeslee et al. 2002) — consistent with the HST Key project value of  $72 \pm 3 \pm 7$  (Freedman et al. 2001) and the WMAP value of  $73_{-3}^{+3}$  (Spergel et al. 2006). For the remaining Virgo cluster galaxy NGC 4342, we used the mean Virgo cluster distance of 17.0 Mpc (Jerjen, Bingeli, & Barazza 2004). The above

three galaxies have slightly different SMBH masses in Table 1 to those in Tremaine et al. (2002) due to the slightly different distances used.

TABLE 1  
GALAXY PARAMETERS

Galaxy	Distance Mpc	$M_{\text{bh}}$ ( $10^8 M_{\odot}$ )	$n$
Elliptical Galaxies			
NGC 821	24.1	$0.85^{+0.35}_{-0.35}$	$4.00^{+0.80}_{-0.67}$
NGC 1399 <sup>a</sup>	20.0	$12^{+5}_{-6}$	$16.8^{+3.36}_{-2.80}$
NGC 3377	11.2	$1.00^{+0.9}_{-0.1}$	$3.04^{+0.61}_{-0.51}$
NGC 3379	10.6	$1.35^{+0.73}_{-0.73}$	$4.29^{+0.86}_{-0.72}$
NGC 4261	31.6	$5.20^{+1.0}_{-1.1}$	$7.30^{+1.46}_{-1.22}$
NGC 4291	26.2	$3.10^{+0.8}_{-2.3}$	$4.02^{+0.80}_{-0.67}$
NGC 4374	18.4	$4.64^{+3.46}_{-1.83}$	$5.60^{+1.12}_{-0.93}$
NGC 4473	15.7	$1.10^{+0.40}_{-0.79}$	$2.73^{+0.55}_{-0.46}$
NGC 4486	16.1	$34.3^{+9.7}_{-9.7}$	$6.86^{+1.37}_{-1.14}$
NGC 4649	16.8	$20.0^{+4.0}_{-6.0}$	$6.04^{+1.21}_{-1.00}$
NGC 4697	11.7	$1.70^{+0.2}_{-0.1}$	$4.00^{+0.80}_{-0.67}$
NGC 5845	25.9	$2.40^{+0.4}_{-1.4}$	$3.22^{+0.64}_{-0.54}$
NGC 6251	$101h_{73}^{-1}$	$5.80^{+1.8}_{-2.0}$	$11.8^{+2.36}_{-1.97}$
NGC 7052	$60h_{73}^{-1}$	$3.40^{+2.4}_{-1.3}$	$4.55^{+0.91}_{-0.76}$
Bulges of Disk Galaxies			
Milky Way <sup>b</sup>	0.008	$0.040^{+0.003}_{-0.003}$	$1.32^{+0.26}_{-0.22}$
NGC 221 <sup>c</sup>	0.81	$0.025^{+0.005}_{-0.005}$	$1.51^{+0.30}_{-0.25}$
NGC 1023	11.4	$0.44^{+0.05}_{-0.05}$	$2.01^{+0.40}_{-0.34}$
NGC 2778 <sup>d</sup>	22.9	$0.14^{+0.08}_{-0.09}$	$1.60^{+0.32}_{-0.27}$
NGC 2787 <sup>e</sup>	7.5	$0.41^{+0.04}_{-0.05}$	$1.97^{+0.39}_{-0.33}$
NGC 3031	3.9	$0.68^{+0.07}_{-0.13}$	$3.26^{+0.65}_{-0.54}$
NGC 3115 <sup>f</sup>	9.7	$9.20^{+3.00}_{-3.00}$	$13.0^{+2.60}_{-2.17}$
NGC 3245	20.9	$2.10^{+0.05}_{-0.05}$	$4.31^{+0.86}_{-0.72}$
NGC 3384 <sup>e</sup>	11.6	$0.16^{+0.01}_{-0.02}$	$1.72^{+0.34}_{-0.29}$
NGC 4258 <sup>g</sup>	7.2	$0.39^{+0.01}_{-0.01}$	$2.04^{+0.41}_{-0.34}$
NGC 4342 <sup>e</sup>	17.0	$3.30^{+1.9}_{-1.1}$	$5.11^{+1.02}_{-0.85}$
NGC 4564 <sup>h</sup>	15.0	$0.56^{+0.03}_{-0.08}$	$3.15^{+0.63}_{-0.53}$
NGC 7457	13.2	$0.035^{+0.011}_{-0.014}$	$1.83^{+0.37}_{-0.31}$

<sup>a</sup>*B*-band image.

<sup>b</sup>2.4- $\mu\text{m}$  minor-axis profile from Kent, Dame, & Fazio (1991).

<sup>c</sup>Taken from Graham (2002).

<sup>d</sup>NGC 2778 is a misclassified S0 galaxy (Rix, Carollo, & Freeman 1999).

<sup>e</sup>HST F814W image.

<sup>f</sup>*I*-band image.

<sup>g</sup>Thuan-Gunn *r* image.

<sup>h</sup>NGC 4564 is a misclassified S0 galaxy (Trujillo et al. 2004).

NOTE.—Distances are taken from Tonry et al. (2001, their table 1), except for the Milky Way (Eisenhauer et al. 2005), NGC 4342 (Virgo cluster distance modulus = 31.15, Jerjen, Binggeli, & Barazza 2004), NGC 6251 ( $v_{\text{CMB}}=7382 \text{ km s}^{-1}$ , Wegner et al. 2003), and NGC 7052 ( $v_{\text{CMB}}=4411 \text{ km s}^{-1}$ , Wegner et al. 2003). These four galaxies are not listed in Tonry et al. (2001). A Hubble constant of  $H_0 = 73 \text{ km s}^{-1} \text{ Mpc}^{-1}$  (Blakeslee et al. 2002; Spergel et al. 2006) has been used for the latter two galaxies. The SMBH masses are from the compilation in Tremaine et al. (2002), except for the Milky Way (Ghez et al. 2003, see also Beloborodov et al. 2006), NGC 821 (Richstone et al. 2006), NGC 3379 (Gebhardt et al. 2000; see also Shapiro et al. 2006), NGC 4486 (Macchetto et al. 1997) and NGC 3115 (Emsellem, Dejonghe, & Bacon 1999). Our sample includes a further three galaxies not listed in Tremaine et al. (2002). The SMBH mass for NGC 3031 and NGC 1399 are from Merritt & Ferrarese (2001a) and Houghton et al. (2006), respectively, and the mass for NGC 4374 is from Maciejewski & Binney (2001, with updated errors taken from Kormendy & Gebhardt 2001). The Sérsic indices are from the major-axis, light-profiles of *R*-band images, except where noted otherwise.

### 3. The $M_{\text{bh}}-n$ correlation

#### 3.1. A linear relation

The  $M_{\text{bh}}-n$  relation presented in Graham et al. (2003a) was constructed using a *bisector* linear regression analysis which treated both variables equally. In that study, the relation was derived with the goal of determining the intrinsic physical relation between  $M_{\text{bh}}$  and the Sérsic shape parameter  $n$  of the bulge. Here our objective is different because we wish to obtain a relation that can be used to *predict* values of  $M_{\text{bh}}$  in other galaxies from their observed bulge Sérsic index  $n$ . We therefore desire an  $M_{\text{bh}}-n$  relation which minimizes the scatter in the quantity to be predicted, and have thus performed an ordinary least squares (OLS) regression of  $M_{\text{bh}}$  on  $n$  for those local galaxies for which both quantities are known (Table 1)<sup>2</sup>.

Following Graham et al. (2003a), we have used a 20 per cent measurement error on the values of  $n$ , or more specifically, we have assigned an error of  $\pm \log(1.2)$  to  $\log(n)$ . Later on we explore the influence of varying this quantity. Several factors can contribute to the size of this term, including errors in the sky-subtraction, uncertainties in the point-spread-function, the presence of bars which are typically not modeled in bulge/disk decompositions, the influence of additional nuclear components such as star clusters or nuclear disks, and partially depleted cores. The latter two issues can be dealt with by either simultaneously fitting a Sérsic function plus some additional function to account for the excess flux above that of the host galaxy (e.g., Graham & Guzmán 2003; Ferrarese et al. 2006a), or with the use of the core-Sérsic model (Graham et al. 2003b; Trujillo et al. 2004). However, due to these various issues, it can be difficult to acquire reliable individual uncertainties on the Sérsic index for every galaxy, hence our use of an average relative error. Similarly, the use of a fixed relative error of 13% and 5% was assigned to the velocity dispersion term used by Merritt & Ferrarese (2001b) and Tremaine et al. (2002), respectively, in their construction of the  $M_{\text{bh}}-\sigma$  relation (with the exception that they both used a 20% uncertainty for the Milky Way’s velocity dispersion).

<sup>2</sup>See Feigelson & Babu (1992) for a clear exposition behind the rationale of when to use what type of regression.

We have used Tremaine et al.’s (2002) modified version of the routine FITEXY (Press et al. 1992), to solve the equation  $y = a + bx$ , by minimising the quantity

$$\chi^2 = \sum_{i=1}^N \frac{(y_i - a - bx_i)^2}{\delta y_i^2 + b^2 \delta x_i^2 + \epsilon^2}. \quad (1)$$

The measurement errors on  $x_i$  and  $y_i$  are denoted by  $\delta x_i$  and  $\delta y_i$ , and the intrinsic scatter  $\epsilon$  is searched for by repeating the fit until  $\chi^2/(N-2)$  equals 1. The uncertainty on  $\epsilon$  is obtained when the reduced chi-squared value,  $\chi^2/(N-2)$ , equals  $1 \pm \sqrt{2/N}$ . Doing so, one obtains

$$\log(M_{\text{bh}}) = 2.69(\pm 0.28) \log(n/3) + 7.81(\pm 0.08), \quad (2)$$

with  $\epsilon = 0.31_{-0.07}^{+0.08}$  dex in  $\log M_{\text{bh}}$ . This fit is shown in Figure 1. The *total* absolute scatter in  $\log M_{\text{bh}}$  is 0.39 dex. Using either an optimistic  $\sim 10\%$  estimate for the uncertainty on  $n$  (specifically, using  $\log[n] \pm \log[1.1]$ ), or a more liberal  $\sim 25\%$  uncertainty (we used  $\log[n] \pm \log[1.25]$ ), see for example Caon, Capaccioli, & D’Onofrio (1993), had no significant ( $1-\sigma$ ) affect on either the slope or intercept of the above relation. The new intrinsic scatter was 0.35 dex and 0.27 dex, respectively.

The maximum  $1-\sigma$  error on the predicted value of  $M_{\text{bh}}$  in galaxies for which  $n$  is known is acquired by assuming uncorrelated errors on  $n$  and the slope and intercept of the  $M_{\text{bh}}-n$  relation. Gaussian error propagation for the linear equation  $y = (b \pm \delta b)(x \pm \delta x) + (a \pm \delta a)$ , gives an error on  $y$  equal to

$$\begin{aligned} \delta y &= \frac{\delta y}{\sqrt{(dy/db)^2(\delta b)^2 + (dy/da)^2(\delta a)^2 + (dy/dx)^2(\delta x)^2}} \\ &= \sqrt{x^2(\delta b)^2 + (\delta a)^2 + b^2(\delta x)^2}. \end{aligned}$$

In the presence of intrinsic variance,  $\epsilon$ , the uncertainty on  $y$  will be greater, such that, assuming the intrinsic variance is in the  $y$  coordinate,

$$\delta y = \sqrt{x^2(\delta b)^2 + (\delta a)^2 + b^2(\delta x)^2 + \epsilon^2}.$$

For our expression (equation 2) we have  $x = \log(n/3)$ , and so  $dx/dn = 1/[\ln(10).n]$ , and therefore

$$\begin{aligned} (\delta \log M_{\text{bh}})^2 &= [\log(n/3)]^2(0.28)^2 + (0.08)^2 \\ &+ [2.69/\ln(10)]^2[\delta n/n]^2 + (0.31)^2. \quad (3) \end{aligned}$$

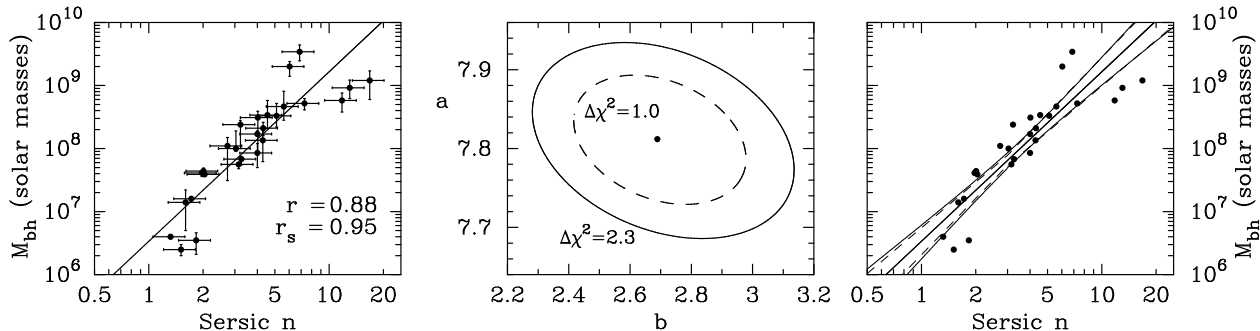


Fig. 1.— Correlation between a galaxy’s supermassive black hole mass and the shape parameter (i.e. Sérsic index  $n$ ) of its dynamically hot component. The Pearson linear correlation coefficient  $r$  is given, as is the Spearman rank-order correlation coefficient  $r_s$ . (The uncertainties on the data points were not used when computing these correlation coefficients.) The regression line shown in the left panel was obtained using a modified version (Tremaine et al. 2002) of the routine FITEXY (Press et al. 1992, their Section 15.3), see equation 2. Consistent results were obtained using the ordinary least squares ( $\log(M_{\text{bh}}) | \log(n/3)$ ) linear-regression routine from Akritas & Bershady (1996), see equation 4. The middle panel shows the  $\Delta\chi^2 = 1.0$  and 2.3 boundaries around the optimal intercept,  $a = 7.81$ , and slope,  $b = 2.69$ . The projection of the  $\Delta\chi^2 = 1.0$  ellipse onto the vertical and horizontal axis gives the  $1\text{-}\sigma$  uncertainties  $\delta a$  and  $\delta b$ , respectively. The  $\Delta\chi^2 = 2.3$  ellipse denotes the  $1\text{-}\sigma$  two-dimensional confidence region. This has been mapped into the right panel, and is traced by the two solid curves. The dashed lines in this panel are the (more commonly used) approximations obtained using  $(a \pm \delta a)$  and  $(b \pm \delta b)$ . The two confidence regions agree well, although the region traced by the dashed lines is, as expected, smaller.

Given the debate over the slope of the  $M_{\text{bh}}\text{-}\sigma$  relation (Merritt & Ferrarese 2001b; Tremaine et al. 2002; Novak et al. 2006), it is of interest to know how much the uncertainty in the slope and intercept of the  $M_{\text{bh}}\text{-}n$  relation may contribute to the uncertainty in the predicted SMBH masses. From equation 3, if one measures a bulge to have  $n = 3$  with  $\delta n/n = 0.2$ , then the error in  $n$  contributes 96% of  $\delta \log M_{\text{bh}}$ . That is, the uncertainty on the slope and intercept of equation 2 are not substantial contributors to the error budget on  $\log M_{\text{bh}}$ . If one has a galaxy with  $n = 1$  or 9, and again  $\delta n/n = 0.2$ , then the combined error from the uncertainty on the slope and intercept contributes only 14% of the error on  $\log M_{\text{bh}}$ .

We have additionally used the OLS regression analysis BCES( $\log M_{\text{bh}} | \log n$ ) from the code of Akritas & Bershady (1996), which allows for both measurement errors and intrinsic scatter. For our sample of  $N = 27$  galaxies, we obtained

$$\log(M_{\text{bh}}) = 2.68(\pm 0.40) \log(n/3) + 7.82(\pm 0.07), \quad (4)$$

with  $\epsilon = 0.30^{+0.09}_{-0.07}$  dex in  $\log M_{\text{bh}}$ . Using an uncertainty of  $\pm \log(1.25)$  or  $\pm \log(1.1)$  for the value of

$\log(n)$  had no significant ( $1\sigma$ ) affect on either the slope or intercept of the above relation — which agrees well with that in equation 2.

### 3.1.1. Symmetrical regression

To obtain the intrinsic astrophysical relation, the modified version of FITEXY which minimizes equation 1 should not be used. The reason is because it is biased — to produce a low slope — by the minimisation of the intrinsic variance,  $\epsilon$ , along the  $y$  (i.e.  $\log M_{\text{bh}}$ ) axis. If the minimisation is instead performed along the  $x$  (i.e.  $\log n$ ) axis, then the  $\epsilon^2$  term in the denominator of equation 1 will be replaced with  $b^2\epsilon^2$ . Making this substitution, and performing the new regression<sup>3</sup>, one obtains  $b = 3.10 \pm 0.33$ ,  $a = 7.78 \pm 0.09$ , and  $\epsilon = 0.11^{+0.04}_{-0.02}$  dex in  $\log n$ .

The average of the above two slopes from the modified FITEXY routine,  $(3.10+2.69)/2 = 2.90$ , agrees well with the slope obtained using the *bisector* linear regression routine BCES from Akritas &

<sup>3</sup>We have ignored unknown, but possible, selection boundaries in  $\log n$  that could bias such a fit (see, e.g., Lynden-Bell et al. 1988, their Figure 10).



Bershady (1996), which gives

$$\log(M_{\text{bh}}) = 2.85(\pm 0.40) \log(n/3) + 7.80(\pm 0.07). \quad (5)$$

This relation is in good agreement with the (intrinsic astrophysical relation) presented in Graham et al. (2003a).

### 3.2. A curved relation

As noted in Graham et al. (2001, 2003a), we have no *a priori* knowledge that the  $M_{\text{bh}}-n$  relation is linear. For this reason, in those papers we employed the use of both linear and non-linear statistics to measure the correlation strength. Here we go one step further by fitting a quadratic to the data.

We stress that, from a physical stand point, we do not know what the actual form of the relation should be. The quadratic equation which we adopt is an empirical model. In a Taylor series expansion it is simply the next order term. The  $M_{\text{bh}}-n$  data may in fact be described by a double power-law, however this would require the use of *four* free parameters (a low- and high-mass slope, and a transition mass and transition Sérsic index). The quadratic relation has only three parameters and is the adopted model for explorations of non-linearity in the  $M_{\text{bh}}-\sigma$  data (Wyithe 2006a,b).

In passing we note that there have been claims that the  $M_{\text{bh}}-\sigma$  relation may not be linear, but has either negative curvature (e.g., Granato et al. 2004; Cirasuolo et al. 2005) positive curvature (e.g. Hopkins & Hernquist 2006), no curvature at even the 0.75-1.5  $\sigma$  level (Wyithe 2006b)<sup>4</sup>, or curves down at low SMBH masses and up at high SMBH masses (Sazonov et al. 2005). Given that the  $L-\sigma$  relation is not linear, having a slope of  $\sim 4$  at the bright end and  $\sim 2$  at the faint end (Tonry 1981; Davies et al. 1983; Held et al. 1992; De Rijcke et al. 2005; Matković & Guzmán 2005), and *if* the  $M_{\text{bh}}-L$  relation *is* linear, then the  $M_{\text{bh}}-\sigma$  relation

<sup>4</sup>The tighter constraint of 0.75  $\sigma$  (that is, the factor in front of a quadratic term is inconsistent with zero at only the 0.75  $\sigma$  level), comes from using SMBHs with resolved sphere's of influence. Including galaxies with unresolved sphere's of influence and adding in single epoch reverberation mapping masses (uncertain to factors of 3-4) weakens the result of a purely linear  $M_{\text{bh}}-\sigma$  relation, with the probability that the second order term does not equal zero ruled out at the (still weak) 1-5-2  $\sigma$  level.

obviously cannot be linear, but must have a positive curvature. Of course, the  $M_{\text{bh}}-L$  relation may not be linear.

We fit the quadratic equation  $y = a + bx + cx^2$ , to the  $(M_{\text{bh}}, n)$  data by minimising the statistic

$$\chi^2 = \sum_{i=1}^N \frac{(y_i - a - bx_i - cx_i^2)^2}{\delta y_i^2 + (2cx_i + b)^2 \delta x_i^2 + \epsilon^2}, \quad (6)$$

where  $y_i = \log(M_{\text{bh},i})$ ,  $x_i = \log(n_i/3)$ , and  $\epsilon$  is the intrinsic variance which, given our objective of predicting new SMBH masses, we attribute entirely to reside in the  $y$  ( $\log M_{\text{bh}}$ ) direction. Solving for  $\chi^2/(N-3) = 1$ , we find

$$\log(M_{\text{bh}}) = 7.98(\pm 0.09) + 3.70(\pm 0.46) \log(n/3) - 3.10(\pm 0.84)[\log(n/3)]^2, \quad (7)$$

with  $\epsilon = 0.18_{-0.06}^{+0.07}$  dex. The total absolute scatter in  $\log M_{\text{bh}}$  is 0.31 dex. From Figure 2, the term  $c$  is inconsistent with a value of zero at greater than the 99.99% confidence level<sup>5</sup>.

With small data sets, formal errors can underestimate the true error on a fitted parameter. To explore the danger that we may be underestimating the uncertainty on the parameter  $c$  in front of the quadratic term in equation 7, we use Bootstrap Monte Carlo simulations. The random number generator **ran1** from Press et al. (2002) was used in a bootstrapping process that involved sampling (with replacement) from the original 27 data points. One thousand data sets containing 27 data points each were then individually fitted to find the optimal log-quadratic equation, exactly as done with the original data. This then gave 1000 new estimates for each of the three parameters ( $a, b, c$ ). The range in values covered by the central 68.3% of these three data sets gives one an estimate of the 1- $\sigma$  confidence intervals — without making any assumption about (the Gaussianity of) the distribution. This parameter range is found to be (7.88...8.04, 3.26...4.24, -3.98...-2.30). This is in good agreement with the 1- $\sigma$  parameter uncertainties obtained from

<sup>5</sup>Excluding the two galaxies with the highest SMBH masses, the total absolute scatter reduces to 0.25 dex, the intrinsic scatter drops to zero, and one finds that  $a = 7.90, b = 3.22$ , and  $c = -2.55$ , only a 1- $\sigma$  deviation from the values obtained using the full data set. Using the full data set, but with the intrinsic scatter set to zero, the value of  $c$  is still inconsistent with a value of zero at the 3- $\sigma$  level.

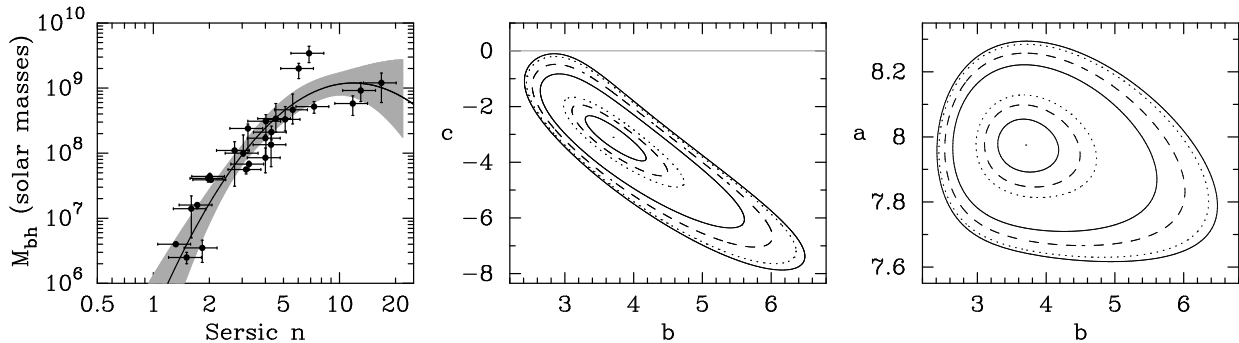


Fig. 2.— Left panel: The data points are the same as in Figure 1, but this time the optimal 3-parameter log-quadratic relation (equation 7) is shown. The absolute scatter in  $\log M_{\text{bh}}$  is 0.31 dex. The shaded area corresponds to the  $\Delta\chi^2 = 3.53$  ( $1\text{-}\sigma$ ) confidence region. Middle and right panel: The inner, central and outer solid contours denote the  $\Delta\chi^2 = 1.00$ , 9.00 and 15.1 boundaries, respectively: their projections onto the vertical and horizontal axes give the 68.3% ( $1\text{-}\sigma$ ) 99.73% ( $3\text{-}\sigma$ ) and 99.99% confidence intervals on the individual parameters in equation 7. The inner and outer dashed lines denote the  $\Delta\chi^2 = 2.30$  and 11.8 boundaries, respectively, delineating the  $1\text{-}\sigma$  and  $3\text{-}\sigma$  two-dimensional confidence regions. The dotted lines show the  $\Delta\chi^2 = 3.53$  and 14.2 boundaries, respectively. They correspond to the  $1\text{-}\sigma$  and  $3\text{-}\sigma$  three-dimensional confidence ellipsoids. (see Press et al. 1992, their Section 15.6).

Figure 2 and given in equation 7. We therefore conclude that we are not under-estimating our errors, and that the  $M_{\text{bh}}\text{-}n$  relation is indeed curved.

Using equation 7, and the value of  $n$  in other galaxies, the maximum error on the predicted value  $\log M_{\text{bh}}$ , denoted by  $\delta \log M_{\text{bh}}$ , can be written as

$$(\delta y)^2 = x^4(\delta c)^2 + x^2(\delta b)^2 + (\delta a)^2 + (2cx + b)^2(\delta x)^2 + \epsilon^2,$$

which equates to

$$(\delta \log M_{\text{bh}})^2 = [\log(n/3)]^4 + [\log(n/3)]^2/4 + (0.09)^2 + [3.70 - 6.20 \log(n/3)]^2[\delta n/n]^2/[\ln(10)]^2 + (0.18)^2(8)$$

Assuming  $\delta n/n = 0.2$ , Table 2 gives the value of  $\delta \log M_{\text{bh}}$  for different values of  $n$ . Obviously the error in the slope of the relation (similarly for the linear relation) causes the masses to be less well constrained at the end of the relation. Due to the steepness of the quadratic relation at low  $n$ , the uncertainty on the estimated SMBH masses can be large there.

In passing we note one of the implications of a curved  $M_{\text{bh}}\text{-}n$  relation. Either the  $M_{\text{bulge}}\text{-}n$  relation must be curved, or the  $M_{\text{bh}}/M_{\text{bulge}}$  ratio can not be constant with mass.

### 3.3. The high-mass end

An obvious consequence of our second order, log-quadratic, relation is the different expected masses at the ends of the relation. For example, at the high mass end, we no longer predict infinitely large SMBHs. Obviously a linear  $M_{\text{bh}}\text{-}n$  relation or a linear  $M_{\text{bh}}\text{-}\sigma$  relation, and a positively curving log-quadratic  $M_{\text{bh}}\text{-}\sigma$  relation, imply infinitely massive SMBH masses at the high- $\sigma$  end. In contrast, our negatively curving  $M_{\text{bh}}\text{-}n$  relation suggests a maximum mass limit to which the universe has built SMBHs<sup>6</sup>. The maximum mass occurs where the derivative of equation 7 equals zero, i.e., where  $d \log(M_{\text{bh}})/d \log(n/3) = 2cx + b = 2(-3.10) \log(n/3) + 3.70 = 0$ . The value of  $n$  at this rather broad peak and turnover is 11.9. Scanning the  $\Delta\chi^2 = 3.53$  ( $1\text{-}\sigma$ ) confidence region shown in Figure 2, so as to provide error bounds, this peak corresponds to a maximum SMBH mass of  $1.2_{-0.4}^{+2.6} \times 10^9 M_{\odot}$ . This upper value matches well with the uppermost mass reported in several observational studies (e.g., McLure et al. 2004; Xie, Zhou, & Liang 2004; Pian, Falomo, & Treves 2005; Sulentic et al. 2006; Kollmeier et al. 2006) and

<sup>6</sup>We do not equate this with a upper mass to which the universe *can* build SMBHS, only with what the universe *has* built.

TABLE 2  
BLACK HOLE MASS UNCERTAINTIES

$n =$	0.5	1.0	2.0	3.0	4.0	8.0	10.0
Linear Fit (equation 2)							
$\log M_{\text{bh}}$	5.72	6.53	7.34	7.81	8.15	8.96	9.22
$\delta \log M_{\text{bh}}$	0.45	0.42	0.40	0.40	0.40	0.41	0.42
Quadratic Fit (equation 7)							
$\log M_{\text{bh}}$	3.22	5.51	7.23	7.98	8.39	8.99	9.07
$\delta \log M_{\text{bh}}$	1.05	0.70	0.47	0.38	0.33	0.36	0.43

NOTE.—Uncertainty,  $\delta \log M_{\text{bh}}$  dex, on an estimated black hole mass using the linear and quadratic  $M_{\text{bh}}-n$  relations as a function of  $n$ . The steepness of the quadratic relation at low  $n$  results in both a better fit to the data for  $1 \leq n \leq 2$ , but also an increased uncertainty on the predicted value of  $\log M_{\text{bh}}$ .

intriguingly with the upper mass limit for axion bubbles (Svidzinsky 2006). We note that this peak is reached somewhat asymptotically as the value of  $n$  increases, and that we do not expect galaxies with larger values of  $n$  to have significantly smaller SMBH masses than the peak mass.

We additionally note that some studies of high-redshift quasars have reported SMBH masses up to  $10^{10} M_{\odot}$ . If correct, such objects would represent a challenge for the quadratic relation defined by the current local sample. Of course, to properly solve this discrepancy requires *direct* SMBH mass measurements. With the upcoming ten-fold increase in spatial resolution (compared to the Hubble Space Telescope), the next generation of extremely large telescopes, such as the Giant Magellan Telescope, will be able to resolve the sphere of influence around SMBHs in galaxies ten times further away. The resultant 1000-fold increase in survey volume should help address the issue of just how massive SMBHs are.

It is also worth remarking that the upper mass limit we find is somewhat of a consequence of our use of a quadratic relation. That is, had we used a four-parameter double power-law, we would not observe such behaviour. Although, Figure 2 does suggest that some kind of asymptotic function,

which reaches a maximum SMBH mass, would also provide a good description to the data. We will, however, postpone a comparison of assorted arbitrary functions for a later time.

The two galaxies with the highest SMBH masses (NGC 4486 and 4649) appear as outliers from the curved relation. We have checked their Sérsic indices are correct and it may be of value to re-examine their black hole masses. While this is beyond the scope of the present paper, we note that there is reason to suspect that NGC 4486 (M87) might have had its black hole mass over-estimated. Maciejewski & Binney (2001) have shown that the SMBH mass in NGC 4374 was reduced by a factor of nearly four, from  $1.7 \times 10^9 M_{\odot}$  to  $4.64 \times 10^8 M_{\odot}$ , after the slit-width was appropriately dealt with. NGC 4486, like NGC 4374, has similarly had its SMBH mass derived from the emissions of a circumnuclear gaseous disk using slit-spectroscopy. These galaxies also appear to have overly large SMBH masses when compared with the theoretical models of Menci et al. (2006, their Figure 1). It may be advantageous to confirm this galaxy’s SMBH mass using AO-assisted integral field spectroscopy with an instruments such as NIFS (McGregor et al. 2003) or SINFONI (Eisenhauer et al. 2003).

### 3.4. The low-mass end

Our negatively curving  $M_{\text{bh}}-n$  relation suggests that the SMBHs in dwarf elliptical galaxies will be smaller than predicted from the linear  $M_{\text{bh}}-n$  relation. When  $n = 1$  ( $M_B \sim -14.5 \pm 1.5$  mag; Graham & Guzmán 2003, their figure 10), one can expect a SMBH mass of  $0.32_{-0.24}^{+0.68} \times 10^6 M_\odot$  and  $3.4_{-1.9}^{+4.1} \times 10^6 M_\odot$  using the quadratic and linear relations, respectively. At  $n = 0.5$  one would expect a SMBH mass of  $1.6_{-1.5}^{+16.8} \times 10^3 M_\odot$  and  $5.2_{-3.1}^{+7.5} \times 10^5 M_\odot$  from the quadratic and linear relations, respectively. When  $n = 0.25$ , the (extrapolated) quadratic relation predicts a mass of only  $\sim 2M_\odot$ . The absence of  $10^5 M_\odot$  black hole detections in local dwarf galaxies (e.g., Valluri et al. 2005) and M33 (Gebhardt et al. 2001; Merritt, Ferrarese, & Joseph 2001) would argue against the extrapolation of the linear relation. The suitability of the curved log-quadratic  $M_{\text{bh}}-n$  relation to globular clusters (e.g., Gebhardt, Rich, & Ho 2005; De Rijcke, Buyle, & Dejonghe 2006, and references therein) remains to be explored.

## 4. Central star clusters

From an analysis of HST images of low-luminosity elliptical galaxies in the Coma cluster, Graham & Guzmán (2003) presented a correlation between the luminosities of nuclear star clusters and that of their host galaxy. Similarly, strong correlations involving Virgo cluster ellipticals have been reported (e.g. Côté et al. 2006) and also between the nuclear star clusters in the bulges of spiral galaxies and their host bulge’s flux (e.g., Balcells et al. 2003). The cluster-to-host flux ratio reported in Graham & Guzman (2003) was a few tenths of one per cent, intriguingly comparable to the mass ratio observed between SMBHs and their host bulge. In Figure 3 we have expanded the  $M_{\text{bh}}-n$  diagram by including the masses of nuclear star clusters plotted against their host galaxy’s Sérsic index. We have used two data sets obtained with the Hubble Space Telescope, and therefore likely to have had a reliable bulge/star-cluster decomposition.

The first data set is from Graham & Guzmán (2003, their Table 2). We have converted their F606W nuclear star cluster magnitudes into masses using an F606W-V color of  $-0.3$  mag (Fukugita, Shimasaku & Ichikawa 1995) and a

V-band mass-to-light ratio  $M/L = 1.5(M_\odot/L_\odot)$ . This ratio is the median of the (King model) dynamical  $M/L$  ratios from 57 star clusters listed in McLaughlin & van der Marel (2005, their Table 13; see also Pryor & Meylan 1993, their Table 2). The second data set comes from Ferrarese et al. (2006a, their Table 3), for which we have used an F475W-V color of 0.2 mag and  $M/L_V = 1.5(M_\odot/L_\odot)$ . Due to the association of SMBHs with their host bulge, rather than the host galaxy, we have excluded the lenticular galaxies<sup>7</sup> because Ferrarese et al. (2006a) modeled the combined bulge+disc light with a single Sérsic function. That is, no bulge/disc decomposition was performed.

Figure 3 reveals (albeit with some scatter which is in part likely due to our conversion from flux to mass) that the nuclear star clusters appear to follow the same log-quadratic relation as defined by the  $(M_{\text{bh}}, n)$  data set. Clearly there is no sharp transition; both SMBHs and star clusters have overlapping masses in the range  $3 \times 10^6 < M_{\text{mco}}/M_\odot < 10^8$ . Furthermore, the lower limit to the SMBH masses may be due to selection effects, i.e., a reflection of our inability to resolve the SMBH sphere of influence in low-mass bulges (Merritt & Ferrarese 2001a). Similar results using host bulge mass, rather than Sérsic index, have recently been reported in Côté et al. (2006), Ferrarese et al. (2006b), Rossa et al. (2006) and Wehner & Harris (2006). McLaughlin, King, & Nayakshin (2006) propose that feedback from supernovae and stellar winds from a nuclear star-cluster can regulate the growth of the host bulge and thereby explain the latter connection.

The result shown in Figure 3 is intriguing because it suggests that the formation mechanisms of nuclear star clusters may share some common processes with the formation of SMBHs. The shallower potential wells, lower central stellar densities (prior to core-depletion in massive elliptical galaxies) and shallower central gradients in lower  $n$  bulges (Terzić & Graham 2005) may result in the production of star clusters rather than SMBHs.

An obvious question is: Do any of the galaxies in Table 1 possess nuclear star clusters in addition to their SMBHs? For the Milky Way the answer

<sup>7</sup>Inclusion of the lenticular galaxies increases the scatter but does not suggest any shift in one particular direction.

is yes (Merritt 2006 and references therein). For the local group galaxy NGC 221 (M32), the excess central flux above the Sérsic model may not represent a distinct additional central massive object, as is the case with the nuclei in NGC 205 (Valluri et al. 2005). In many galaxies, the presence of non-thermal flux from AGN can complicate the identification of nuclear star clusters when using only images and light-profiles. One additionally requires spectral information. In general, core-Sérsic galaxies do not show any excess nuclear flux, and the few which do show excess flux have an AGN. In contrast, the majority of the lower-luminosity Sérsic (“power-law”) galaxies in Table 1 *do* show excess nuclear flux. However, this is usually due to an AGN. Two exceptions are NGC 3384 and NGC 7457, which possess both a SMBH *and* a central star cluster (Ravindranath et al. 2001).

While the mass of the star cluster in NGC 3384 is approximately twice its SMBH mass, the star cluster in NGC 7457 is an order of magnitude greater than its SMBH mass<sup>8</sup> Creating a new  $M_{\text{bh+mco}}-n$  diagram would move NGC 7457 (which has the second lowest SMBH mass in our sample) so that it overlaps with a cluster of three other data points seen in Figure 2 — leaving it consistent with the quadratic shown there.

Successive mergers of nucleated, low- $n$ , low-luminosity galaxies will eventually result in a galaxy whose mass is sufficient to expect a SMBH. This then raises the tantalising possibility of the *recent* formation of some SMBHs from the merger of two, or more, nucleated galaxies and the subsequent merger and ‘runaway collision’ of their respective nuclear star clusters. To date, such a collisional process in star clusters has only been invoked to explain the formation of intermediate-mass black holes (IMBHs: Quinlan & Shapiro 1990; Portegies Zwart et al. 1999; Freitag, Gürkan, & Rasio 2006). We are, however, unaware of the actual dwarf-dwarf galaxy collision rate today, and do not wish to suggest it is a frequent phenomenon.

The formation scenario proposed here for potential *young* SMBHs is perhaps, at face value,

<sup>8</sup>The apparent  $H$ -band magnitudes were converted into absolute magnitudes using the distances in Table 1, and then into units of solar luminosity using  $M_{\odot,H}=3.32$  (Bessell, Castelli, & Plez 1998, their Appendix C and D), and finally solar mass using  $M/L_H = 1.0(M_{\odot}/L_{\odot})$ .

contrary to the conventional scenario in which they form via gas accretion during the height of quasar activity. Indeed, massive black holes have long been known to exist at high-redshifts,  $z > 3$ . Nonetheless, we do not rule out a kind of “down-sizing” or late-time formation of low-mass SMBHs built through a relatively dry runaway merger of nuclear star clusters. While involving no significant AGN feedback, such a process could still maintain the  $M_{\text{mco}}/M_{\text{bulge}}$  mass ratio.

If there are appreciable numbers of *young* SMBHs built from the merger of nuclei, this may require a downward revision to measurements of the average radiative efficiency of SMBHs and thus their implied rate of rotation (e.g., Ferrarese 2002; Shankar et al. 2004; Wang et al. 2006).

## 5. Dependence on $H_0$

The above linear and curved relations are nearly, but not completely, independent of the Hubble constant. While the Sérsic indices are independent of galaxy distance, the SMBH masses depend linearly on the distance to each galaxy. Distances for 24 of our 27 galaxies were obtained from surface brightness fluctuation measurements and are thus independent of the Hubble constant, as of course is the Milky Way center. However, a Hubble constant of  $73 \text{ km s}^{-1} \text{ Mpc}^{-1}$  was used to derive the distances to NGC 6251 and NGC 7052 from their redshift.

Studies which use the  $M_{\text{bh}}-n$  relation, or indeed the  $M_{\text{bh}}-\sigma$  relation, need to know if the SMBH masses predicted from the relation are dependent on  $H_0$ . If they are, then the Hubble constant needs to be factored into such mass derivations and thus also estimates of the SMBH mass function and space density. We have therefore rederived the quadratic  $M_{\text{bh}}-n$  relation excluding NGC 6251 and NGC 7052, so as to remove any possible dependency on  $H_0$ . Doing so, we obtain  $\log(M_{\text{bh}}) = 7.97(\pm 0.09) + 3.75(\pm 0.46) \log(n/3) - 2.92(\pm 0.83)[\log(n/3)]^2$ , with  $\epsilon = 0.17_{-0.06}^{+0.09}$  dex.

This is not significantly different from the expression given in equation 7. In fact, the main reason for the slight shift in numbers is because of the exclusion of NGC 6251 — which resides at the high- $n$  end of the relation, and thus has more weight than individual points in the middle of the relation — rather than the use of  $H_0 = 73 \text{ km}$

$\text{s}^{-1} \text{Mpc}^{-1}$  for this galaxy. This is evidenced by using  $H_0 = 100 \text{ km s}^{-1} \text{Mpc}^{-1}$  for NGC 6251 and NGC 7052 and adjusting their SMBH masses accordingly, which results in  $\log(M_{\text{bh}}) = 7.97 + 3.64 \log(n/3) - 3.11[\log(n/3)]^2$ . This expression is closer to equation 7 than the expression in the previous paragraph is to equation 7, and reveals that the exclusion of NGC 6251 and NGC 7052 introduces more of a change than the use of an uncertain Hubble constant. It therefore makes sense to use equation 7 and, given the uncertainties on the fitted parameters  $a, b$  and  $c$ , treat equation 7 as if it were independent of the Hubble constant. The same statement is true for equations 2, 4 and 5.

## 6. An $M_{\text{bh}}-\mu_0$ relation

There are now several relations between SMBH mass and the properties of the host bulge, such as luminosity, mass, velocity dispersion within some radius, and concentration. Which of these is the most fundamental remains unanswered (Novak et al. 2006). It may be that none of these are the drivers of the SMBH-bulge connection, but that all are symptomatic of a more profound relation. For instance, the combination of concentration and central density might be what is important — as this defines both the baryonic distribution and the strength of the gravitational potential with radius, at least until dark matter becomes a significant factor. It is therefore not unreasonable to expect that this might influence, or possibly even dictate, the ability of a bulge to fuel any central SMBH.

The motion of the stars within a bulge, traced through the observable  $\sigma$ , is the dynamical *response* to the underlying mass distribution. While  $\sigma$  is therefore a tracer of mass, it is obviously dependent on how that mass is distributed, and is thus a) a function of the central stellar density and b) has a radial dependence which is set by the stellar concentration, at least within  $\sim 1R_e$  (Lintott, Ferreras, & Lahav 2006).

While the SMBH mass might be a product of the radial mass distribution, specified by the central density and concentration, the observed relation between central density and concentration (e.g., Graham & Guzmán 2003, their Figure 9; Merritt 2006, his Figure 5) subsequently means that one can express the SMBH mass in terms of just one of these quantities. Extrapolating

under the nuclear star clusters in low-luminosity bulges, and over the partially-depleted cores in giant galaxies — whose central stellar density has been modified by the slingshot effect of coalescing SMBHs — gives an estimate of a bulge’s (original) central stellar density. Given the  $M_{\text{bh}}-n$  relations derived in this paper, we can predict a correlation between  $M_{\text{bh}}$  and central stellar density.

Substituting  $\log(n) = (22.8 - \mu_{0,B})/14$ , where  $\mu_{0,B}$  is the central  $B$ -band surface density (Graham & Guzmán 2003)<sup>9</sup>, into equation 2 gives

$$\log(M_{\text{bh}}) = 10.91 - 0.19\mu_{0,B}. \quad (9)$$

A relatively large uncertainty on the central surface brightness of  $1 \text{ mag arcsec}^{-2}$  translates to an uncertainty of only 0.19 dex in the logarithm of the SMBH mass, a value comparable to the intrinsic scatter found for equation 7. Substitution of the above term for  $\log(n)$  into equation 7 gives

$$\log(M_{\text{bh}}) = 8.13 + 0.25\mu_{0,B} - 0.016(\mu_{0,B})^2. \quad (10)$$

These two expressions differ most in their prediction of SMBH masses at the low mass end (Figure 4), with the linear relation predicting  $\sim 10^6 M_\odot$  masses if  $\mu_0 = 25B\text{-mag}$ , and the quadratic relation predicting masses of  $\sim 10^4 M_\odot$  at this faint central surface brightness.

Although we are unable to conclude that an  $M_{\text{bh}}-\mu_0$  relation is more, or even equally, fundamental than any other relation involving SMBH mass, we do consider it prudent to explore this possibility. We hope to acquire calibrated, high-resolution, near-infrared images to further investigate this proposed relation. Due to the random projection angles of triaxial bulges on the plane of the sky, one might expect a certain amount of variability in the observed values of  $\mu_{0,B}$ . We therefore note that it may be advantageous to construct a plot of SMBH versus the deprojected (internal) central density. Such a program, however, is beyond the intended scope of this paper.

## 7. Summary

We have constructed the  $M_{\text{bh}}-n$  relation using updated SMBH masses and refined galaxy

<sup>9</sup>Many of our images are photometrically uncalibrated, so we are unable to plot  $\log(M_{\text{bh}})$  versus  $\mu_0$  with the present data set.

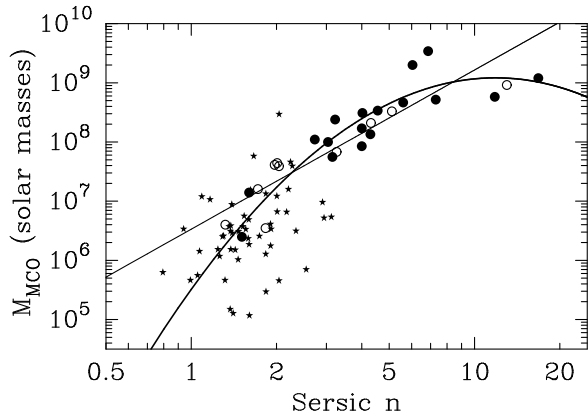


Fig. 3.— Central ‘massive compact object’ mass versus host galaxy Sérsic index ‘ $n$ ’. Filled circles represent SMBHs in elliptical galaxies, while open circles represent SMBHs in disk galaxies. The stars represent nuclear star clusters in elliptical galaxies presented in Graham & Guzmán (2003) and Ferrarese et al. (2006). The straight line is the same as that shown in Figure 1, and the curved line is the same as that shown in Figure 2.

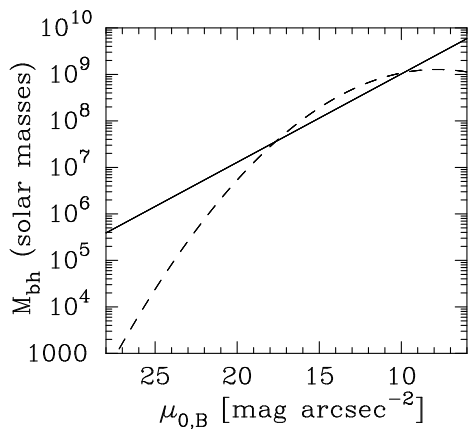


Fig. 4.— Predicted correlation between SMBH mass and the central  $B$ -band surface brightness of the host bulge, after allowing for excess nuclear flux and partially-depleted cores, as mentioned in Section 6. The solid line corresponds to equation 9, the dashed line corresponds to equation 10.

light-profile shapes,  $n$ . We performed an ordinary least squares, linear regression of  $M_{\text{bh}}$  on  $n$  that allows for measurement errors and intrinsic scatter  $\epsilon$ , to obtain  $\log(M_{\text{bh}}) = 7.81(\pm 0.08) + 2.69(\pm 0.28) \log(n/3)$ , with  $\epsilon = 0.31_{-0.07}^{+0.09}$  dex in  $\log M_{\text{bh}}$ .

We additionally considered the possibility that the  $M_{\text{bh}}-n$  relation may not be linear, and applied a quadratic fit to account for the apparent curvature in the distribution. Although an arbitrary empirical function, the second order term in the quadratic fit

$$\log(M_{\text{bh}}) = 7.98(\pm 0.09) + 3.70(\pm 0.46) \log(n/3) - 3.10(\pm 0.84) [\log(n/3)]^2,$$

with an intrinsic scatter  $\epsilon = 0.18_{-0.06}^{+0.07}$  dex, is inconsistent with a value of zero at the 99.99% confidence level. These relations were constructed with the objective of obtaining a relation that can be used to predict SMBH masses in other galaxies for which the bulge Sérsic index is known. Unlike the linear relation, the quadratic relation predicts finite SMBH masses at the high- $n$  end, and  $\sim 10^3 M_{\odot}$  mass black holes when  $n \sim 0.5$ , rather than  $\sim 10^5 M_{\odot}$  obtained with the linear relation.

The Sérsic index, a quantity obtained from uncalibrated images, and independent of galaxy distance, offers an easy way to acquire accurate estimates of black hole masses in other galaxies. Moreover, the strength of the correlation ( $r = 0.88$ ,  $r_s = 0.95$ ) implies a fundamental connection that theory is yet to explain. In addition, we have shown that the nuclear star clusters at the centers of low-luminosity bulges appear to follow the same log-quadratic  $M_{\text{bh}}-n$  relation. This is suggestive, although not conclusive, that a similar formation mechanism may be responsible for the build up of massive compact objects (whether black holes or star clusters) at the centers of bulges.

Finally, in Section 6 we have derived, for the first time, the expected linear and quadratic relation connecting the mass of a SMBH with the central surface brightness of its host bulge (Figure 4).

We are grateful to Rebecca Koopmann who kindly supplied us with data for NGC 4649 (Koopmann, Kenney, & Young 2001), and to Helmut Jerjen who provided light-profiles for NGC 3115,

NGC 4486, NGC 4649, and NGC 4697. The light-profile for NGC 4564 was originally obtained by Peter Erwin as a part of Graham et al. (2001). We thank Eric Feigelson and Charles Jenkins for the statistical advice they provided early on in this work. We also thank Stuart Wyithe for his comments and kindly supplying us with a code which we subsequently modified to fit a quadratic to our data set. This research has been supported by the Australian Research Council through Discovery Project Grant DP0451426. This research has made use of the NASA/IPAC Extragalactic Database (NED), the Isaac Newton Group and HST data archives, and StatCodes available at (<http://www.astro.psu.edu/statcodes/>).

## REFERENCES

- Akritas, M.G., & Bershadsky, M.A., 1996, *ApJ*, 470, 706
- Allen, P., Driver, S.P., Graham, A.W., Cameron, E., Liske, J., & De Propris, R., 2005, *MNRAS*, submitted
- Balcells, M., Graham, A.W., Domínguez-Palmero, L., & Peletier, R.F. 2003, *ApJ*, 582, L79
- Beloborodov, A.M., Levin, Y., Eisenhauer, F., Genzel, R., Paumard, T., Gillessen, S., & Ott, T., 2006, *ApJ*, submitted (astro-ph/0601273)
- Bessell, M.S., Castelli, F., & Plez, B. 1998, *A&A*, 333, 231
- Blakeslee, J.P., et al., 2002, *MNRAS*, 330, 443
- Broderick, A.E., & Narayan, R., 2006, *ApJ*, 638, L21
- Caon, N., Capaccioli, M., & D’Onofrio, M., 1993, *MNRAS*, 265, 1013
- Caon, N., Capaccioli, M., & D’Onofrio, M., 1994, *A&AS*, 106, 199
- Cappellari, M., Verolme, E.K., van der Marel, R.P., Verdoes Kleijn, G.A., Illingworth, G.D., Franx, M., Carollo, C.M., & de Zeeuw, P.T., 2002, *ApJ*, 578, 787
- Cheng, K.P., et al. 1997, *UITVi*; Vol. U
- Cirasuolo, M., Shankar, F., Granato, G.L., de Zotti, G., & Danese, L., 2005, *ApJ*, 629, 816
- Côté, P., et al. 2006, *ApJS*, in press (astro-ph/0603252)
- Cross, N.J.G., Driver, S.P., Liske, J., Lemon, D.J., Peacock, J.A., Cole, S., Norberg, P., & Sutherland, W.J., 2004, *MNRAS*, 349, 576
- Davies, R.L., Efstathiou, G., Fall, M., Illingworth, G., & Schechter, R.L. 1983, *AJ*, 266, 41
- De Rijcke, S., Buyle, P., & Dejonghe, H. 2006, *MNRAS*, in press (astro-ph/0601450)
- De Rijcke, S., Michielsen, D., Dejonghe, H., Zeilinger, W.W., & Hau, G.K.T. 2005, *A&A*, 438, 491
- D’Onofrio, M., Capaccioli, M., & Caon, N. 1994, *MNRAS*, 271, 523
- Driver, S.P., Allen, P.D., Graham, A.W., Cameron, E., Liske, J., Ellis, S.C., Cross, N.J.G., De Propris, R., Phillips, S., & Couch, W.J., 2006, *MNRAS*, 368, 414
- Eisenhauer, F., et al., 2003, *SPIE*, 4841, 1548
- Eisenhauer, F., et al., 2005, *ApJ*, 628, 246
- Emsellem, E., Dejonghe, H., Bacon, R., 1999, *MNRAS*, 303, 495
- Erwin, P., Graham, A., & Caon, N., 2002, in “Carnegie Observatories Astrophysics Series, Vol.1: Coevolution of Black Holes and Galaxies,” ed. L.C. Ho (Pasadena: Carnegie Observatories) (astro-ph/0212335)
- Erwin, P., Beltrán, J.C.V., Graham, A.W., & Beckman, J.E. 2003, *ApJ*, 597, 929
- Feigelson, E.D., Babu, G.J., 1992, *ApJ*, 397, 55
- Ferrarese, L., 2002, in *Proc. 2nd KIAS Astrophysics Workshop, Current High-Energy Emission around Black Holes*. Ed. C.-H.Lee. World Scientific, Singapore (astro-ph/0203047)
- Ferrarese, L., & Ford, H.C., 2005, *Space Science Reviews*, 116, 523 (astro-ph/0411247)
- Ferrarese, L., & Merritt, D., 2000, *ApJ*, 539, L9
- Ferrarese, L., et al., 2006a, *ApJS*, in press (astro-ph/0602297)
- Ferrarese, L., et al., 2006b, *ApJL*, accepted (astro-ph/0603840)
- Forbes, D.A., & Reitzel, D.B., 1995, *AJ*, 109, 1576
- Freedman, W., et al., 2001, *ApJ*, 553, 47
- Frei, Z., Guhathakurta, P., Gunn, J.E., & Tyson, J.A., 1996, *AJ*, 111, 174



- Freitag, M., Gürkan, M.A., & Rasio, F.A. 2006, MNRAS, 324, 141
- Fukugita, M., Shimasaku, K., & Ichikawa, T. 1995, PASA, 107, 945
- Gebhardt, K., et al., 2000, AJ, 119, 1157
- Gebhardt, K., et al., 2001, AJ, 122, 2469
- Gebhardt, K., Rich, R.M., & Ho, L., 2005, ApJ, 634, 1093
- Ghez, A.M., et al., 2003, ApJ, 586, L127
- Ghez, A.M., et al., 2005, ApJ, 620, 744
- Graham, A.W., 2002, MNRAS, ApJ, 568, L13
- Graham, A.W., Colless, M.M., & Busarello, G. 1998, ASP Conf. Ser. 136: Galactic Halos, 136, 257
- Graham, A.W., & Driver, S.P., 2005, PASA, 22(2), 118 (astro-ph/0503176)
- Graham, A.W. Erwin, P., Caon, N., & Trujillo, I., 2001, ApJ, 563, L11
- Graham, A.W. Erwin, P., Caon, N., & Trujillo, I., 2003a, in Galaxy Evolution: Theory and Observations, RevMexAA (SC), eds., V. Avila-Reese, C. Firmani, C.S. Frenk, & C. Allen, vol. 17, 196-197
- Graham, A.W. Erwin, P., Trujillo, I., & Asensio Ramos, A., 2003b, AJ, 125, 2951
- Graham, A.W., & Guzmán, R., 2003, AJ, 125, 2936
- Granato, G.L., De Zotti, G., Silva, L., Bressan, A., & Danese, L., 2004, ApJ, 600, 580
- held, E.V., de Zeeuw, T., Mould, J., & Picard, A. 1992, AJ, 103, 851
- Häring, N., & Rix, H.-W., 2004, ApJ, 604, L89
- Hopkins, P.F., & Hernquist, L. 2006, ApJS, submitted (astro-ph/0603180)
- Houghton, R.C.W., Magorrian, J., Sarzi, M., Thatte, N., & Davies, R.L. 2006, MNRAS, in press
- Jerjen, H., Binggeli, B., & Barazza, F.D., 2004, AJ, 127, 771
- Jerjen, H., Kalnajs, A., & Binggeli, B. 2000, A&A, 358, 845
- Kahaner, D., Moler, C., & Nash, S. 1989, Numerical Methods and Software, Englewood Cliffs: Prentice Hall, 1989
- Kent, S.M., Dame, T., & Fazio, G., 1991, ApJ, 378, 131
- Kollmeier, J.A., et al. 2006, ApJ, 648, 128
- Koopmann, R.A., Kenney, J.D.P., & Young, J., 2001, ApJS, 135, 125
- Kormendy, J., 1993, in The Nearest Active Galaxies, ed. J.E.Beckman, L.Colina, & H.Netzer (Madrid: CSIC), 197
- Kormendy, J., & Gebhardt, K., 2001, in The 20th Texas Symposium on Relativistic Astrophysics, ed. H. Martel, & J.C. Wheeler, AIP, 586, 363
- Kuchinski, L.E., et al. 2000, ApJS, 131, 441
- Lintott, C.J., Ferreras, I., Lahav, O. 2006, ApJ, 648, 826
- Liske, J., Lemon, D.J., Driver, S.P., Cross, N.J.G., & Couch, W.J., 2003, MNRAS, 344, 307
- Lynden-Bell, D., et al., 1988, ApJ, 326, 19
- Macchetto, F., Marconi, A., Axon, D.J., Capetti, A., Sparks, W., & Crane, P., 1997, ApJ, 489, 579
- Maciejewski, W., & Binney, J., 2001, MNRAS, 323, 831
- Magorrian, J., et al., 1998, AJ, 115, 2285
- Malin, D.F., 1985, in New Aspects of Galaxy Photometry, ed. J.-L. Nieto (Berlin: Springer), 27
- Marconi, A., & Hunt, L.K., 2003, ApJ, 589, L21
- Matković, A., & Guzmán, R., 2005, MNRAS, 362, 289
- McGregor, P.J., et al. 2003, SPIE, 4841, 1581
- McLaughlin, D.E., King, A.R., & Nayakshin, S. 2006, ApJL, in press (astro-ph/0608521)
- McLaughlin, D.E., & van der Marel, R.P. 2005, ApJS, 161, 304
- McLure, R.J., & Dunlop, J.S., 2002, MNRAS, 331, 795
- McLure, R.J., Willott, C.J., Jarvis, M., Rawlings, S., Hill, G.J., Mitchell, E., Dunlop, J.S., & Wold, M., 2004, MNRAS, 351, 347
- Menci, N., Fontana, A., Giallongo, E., Grazian, A., & Salimbeni, S. 2006, ApJ, in press (astro-ph/0605123)
- Merritt, D. 2006, in Reports on Progress in Physics, D69, 2513

- Merritt, D., & Ferrarese, L., 2001a, in *The Central kpc of Starbursts and AGN*, ASP Conf. Ser., 249, 335
- Merritt, D., & Ferrarese, L., 2001b, *ApJ*, 547, 140
- Merritt, D., Ferrarese, L., & Joseph, C.L. 2001, *Science*, 293, 1116
- Miller, M.C., 2006, *MNRAS*, in press (astro-ph/0512194)
- Miyoshi, M., Moran, J.m Herrnstein, J., Greenhill, L., Nakai, N., Diamond, P., & Inoue, M., 1995, *Nature*, 373, 127
- Novak, G.S., Faber, S.M., & Dekel, A., 2006, *ApJ*, 637, 96
- Pian, E., Falomo, R., & Treves, A., 2005, *MNRAS*, 361, 919
- Portegies Zwart, S.F., Makino, J., McMillan, S.L.W., & Hut, P. 1999, *A&A*, 348, 117
- Press, W.H., Teukolsky, S.A., Vetterling, W.T., & Flannery, B.P., 1992, *Numerical recipes* (2nd ed.; Cambridge: Cambridge Univ. Press)
- Pryor, C., & Meylan, G. 1993, ASP Conf. Ser. 50: *Structure and Dynamics of Globular Clusters*, 50, 357
- Quinlan, G.D., & Shapiro, S.L. 1990, *ApJ*, 356, 483
- Ravindranath, S., Ho, L.C., Peng, C.Y., Filippenko, A.V., & Sargent, W.L.W. 2001, *AJ*, 122, 653
- Richstone et al., et al., 2006, *ApJL*, submitted (astro-ph/0403257)
- Rix, H.-W., Carollo, C.M., & Freeman, K., 1999, *ApJ*, 513, L25
- Rossa, J., et al. 2006, *AJ*, submitted (astro-ph/0604140)
- Salucci, P., Szuszkiewicz, E., Monaco, P., & Danese, L., 1999, *MNRAS*, 307, 637
- Sazonov, S.Yu., Ostriker, J.P., Ciotti, L., & Sunyaev, R.A., 2005, *MNRAS*, 358, 168
- Schödel, R., Ott, T., Genzel, R., Eckart, A., Mouawad, N., & Alexander, T. 2003, *ApJ*, 596, 1015
- Sérsic, J.-L., 1963, *Boletin de la Asociacion Argentina de Astronomia*, vol.6, p.41
- Shankar, F., Salucci, P., Granato, G.L., De Zotti, G., & Danese, L., 2004, *MNRAS*, 354, 1020
- Shapiro, K.L., Cappellari, M., de Zeeuw, T., McDermid, R.M., Gebhardt, K., van den Bosch, R.C.E., Statler, T.S. 2006, *MNRAS*, 370, 559
- Spergel, D.N., et al. 2006, *ApJ*, submitted (astro-ph/0603449)
- Sulentic, J.W., Repetto, P., Stirpe, G.M., Marziani, P., Dultzin-Hacyan, D., & Calvani, M., 2006, *A&A*, 456, 929
- Svidzinsky, A.A. 2006 (astro-ph/0607179)
- Terzić, B., & Graham, A.W. 2005, *MNRAS*, 362, 197
- Tonry, J.L. 1981, *ApJ*, 251, 1
- Tonry, J.L., et al., 2001, *ApJ*, 546, 681
- Tremaine, S., et al., 2002, *ApJ*, 574, 740
- Trujillo, I., Erwin, P., Asensio Ramos, A., & Graham, A.W., 2004, *AJ*, 127, 1917
- Valluri, M., Ferrarese, L., Merritt, D., & Joseph, C.L., 2005, *ApJ*, 628, 137
- Wang, J.-M., Chen, Y.-M., Ho, L.C., & McLure, R.J. 2006, *ApJ*, 642, L111
- Wegner, G., et al., 2003, *AJ*, 126, 2268
- Wehner, E.H., & Harris, W.E. 2006, *ApJL*, submitted (astro-ph/0603801)
- Wyithe, J.S.B., 2006a, *MNRAS*, 365, 1082
- Wyithe, J.S.B., 2006b, *MNRAS*, 371, 1536
- Xie, G.Z., Zhou, S.B., & Liang, E.W., 2004, *AJ*, 127, 53
- Yu, Q., Tremaine, S., 2002, *MNRAS*, 335, 965

## 8. APPENDIX A: Galaxy light-profiles

We have made use of the  $R$ -band galaxy images of NGC 4486, NGC 4564, NGC 4649, and NGC 4697 taken by Cheng et al. (1997), Frei et al. (1996), Kuchinski et al. (2000), and HST/ACS archive Proposal ID 10003 (PI C.Sarazin), respectively. In the case of NGC 3115 we used an  $I$ -band image from Kuchinski et al. (2000), and for the Milky Way we used the near-infrared light-profile from Kent, Dame, & Fazio (1991).

For the  $R$ -band images, the light-profiles were obtained in the standard way. Foreground stars and background galaxies were carefully masked, and the sky-background flux was determined from the mean of  $\sim 10$  median fluxes that were obtained from small boxes we positioned near the (galaxy-free) corners of each chip. The light-profiles were extracted using the IRAF task ELLIPSE, with the isophotal position angle and ellipticity free to vary, but the centroid fixed.

An interesting deviation from the above recipe pertains to the analysis of the edge-on S0 galaxy NGC 3115. Its light-profile was obtained using another isophotal fitting routine written in IRAF (Jerjen, Kalnajs & Bingelli 2000). After the foreground and background objects, and non-symmetrical features about the nominal galaxy centre, were removed from the image, a symmetrical two-dimensional (2D) model was constructed from the remaining light distribution by allowing the isophotal ellipticity and position angle to vary, but keeping the luminosity-weighted centre fixed. This process was repeated iteratively until the residuals were minimised. This left a residual image displaying only the edge-on disc of NGC 3115. The one-dimensional surface brightness profile of the (symmetrical) bulge was then calculated from this 2D model.

Foreground stars were fitted with a Moffat function that was used to quantify the point spread function in each image. However, in practice this wasn't important because in avoiding the potential presence of nuclear star clusters or partially-depleted cores, we first removed the inner  $\sim 2$  seeing disks from the galaxy light-profiles before fitting Sérsic's (1963) function.

Each light-profile's best-fitting Sérsic  $R^{1/n}$  function plus, in the case of NGC 4564, an exponential disk, was obtained using the subroutine

UNCMND from Kahaner, Moler & Nash (1989). At each iteration, the nonlinear (seeing-convolved) Sérsic function (plus exponential function when modelling NGC 4564) was approximated by a quadratic function derived from a Taylor series. The quadratic function was minimised to obtain a search direction, and an approximate minimum of the nonlinear function along the search direction found using a line search. The algorithm computes an approximation to the second derivative matrix of the nonlinear function using quasi-Newton techniques. The galaxy light-profiles and best-fitting models are displayed in Figures 5 and 6. One can see, particularly from the residual profiles in the lower panels, that the fitted models perform well at matching the curvature in the light-profiles. This curvature, specifically, the Sérsic index  $n$ , is observed to correlate strongly with a bulge's central supermassive black hole (e.g., Figure 2).

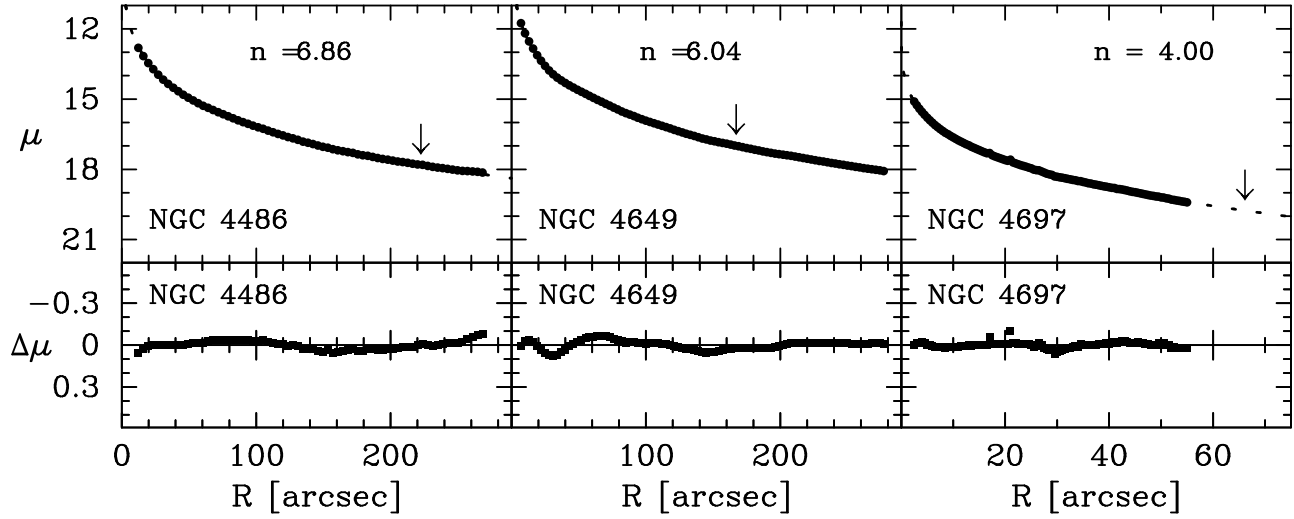


Fig. 5.— Major-axis  $R$ -band light-profiles for three elliptical galaxies with directly measured SMBH masses. The best-fitting Sérsic function is shown by the solid curve. The arrows mark the spheroids' half-light radii. The residuals of the data about the fit are shown in the lower panels. (Note: Due to the fact that the  $M_{\text{bh}}-n$  relation does not require calibrated images, the profiles have not had their photometric zero-point determined.)

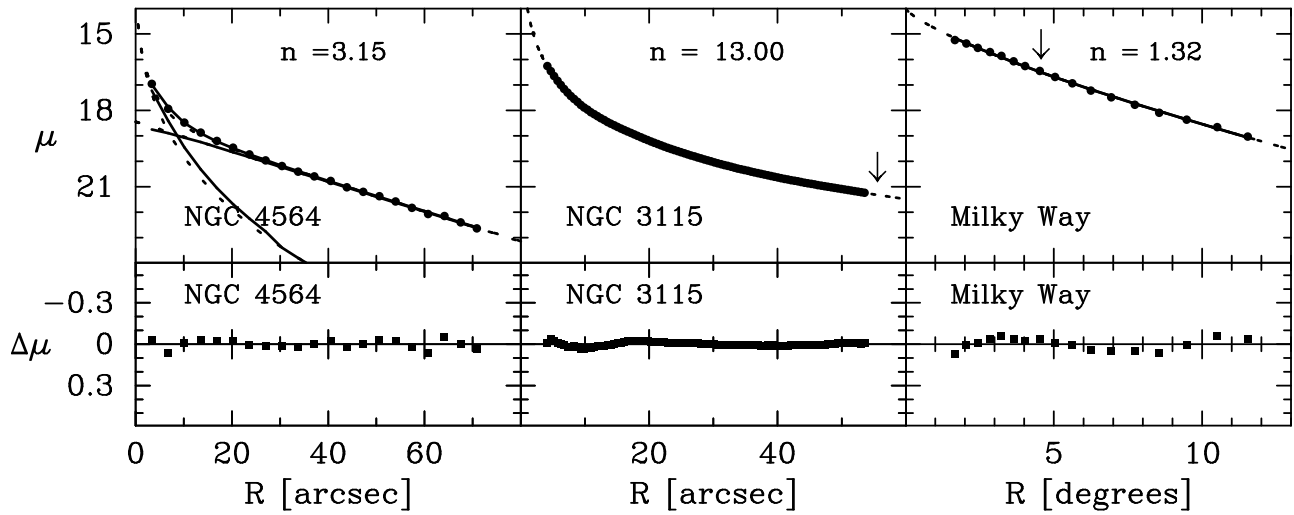


Fig. 6.— Major-axis light-profile for the disk galaxy NGC 4564, the bulge of the edge-on lenticular galaxy NGC 3115, and the bulge of the Milky Way. The best-fitting Sérsic function (and exponential) are shown by the curved lines (and the straight lines). The solid lines show the seeing-convolved functions; the dashed lines show the unconvolved functions, i.e., the intrinsic profile. (Note: Due to the fact that the  $M_{\text{bh}}-n$  relation does not require calibrated images, the profiles have not had their photometric zero-point determined.)